

Increasing synchronization may promote seizure termination: Evidence from status epilepticus

Kaspar Schindler ^{a,*}, Christian E. Elger ^a, Klaus Lehnertz ^{a,b,c}

^a Klinik für Epileptologie, University of Bonn, Sigmund-Freud-Str. 25, 53105 Bonn, Germany

^b Helmholtz-Institut für Strahlen- und Kernphysik, University of Bonn, Nussallee 14-16, 53115 Bonn, Germany

^c Interdisciplinary Center for Complex Systems, University of Bonn, Römerstr. 164, 53117 Bonn, Germany

Accepted 10 June 2007

Abstract

Objective: To test whether increasing synchronization of neuronal activity might be causally related to seizure termination.

Methods: Neuronal synchronization was assessed by the relative changes of the eigenvalue spectrum of the equal-time correlation matrix computed from a short window sliding along multi-channel EEGs, recorded with either intracranial or surface electrodes.

Results: Synchronization dynamics of six status epilepticus EEG recordings from six patients were assessed. In all six recordings EEG synchronization fluctuated around relatively low levels during ongoing epileptiform activity. Synchronization only persistently increased before, or in one case, at the end of status epilepticus. Ongoing seizure activity stopped without pharmacological intervention in one patient. In four of the five other cases, the persistent increase of synchronization followed administration of anticonvulsant drugs.

Conclusions: Our findings support the hypothesis that increasing synchronization of neuronal activity may be considered as an emergent self-regulatory mechanism for seizure termination.

Significance: The traditional concept is challenged that increasing neuronal synchronization during epileptic seizures is always pathological and should be suppressed. On the contrary, our findings imply that therapeutic interventions to increase synchronization during seizures might be beneficial.

© 2007 International Federation of Clinical Neurophysiology. Published by Elsevier Ireland Ltd. All rights reserved.

Keywords: Seizure termination; Synchronization; Status epilepticus; EEG; Drug action; Brain stimulation

1. Introduction

Epileptic seizures are generated by the collective activity of extended neuronal networks. They are often referred to as “pathologically hypersynchronized states”. This vague notion fosters the intuitive concept that seizure termination may be induced by desynchronization (Milton and Jung, 2003), which, however, may turn out to be a misleading conclusion. The problem is that the term “hypersynchronization” should not be used without indicating the spatial scale one is referring to. We have recently demonstrated that on the spatial scale assessed

by multi-channel intracranial EEG, the zero-lag correlation remains approximately unchanged or – in the case of secondary generalization – decreases only during the first half of the seizures, but then gradually increases before seizures terminate (Schindler et al., 2007). This development was qualitatively independent of the anatomical location of seizure onset zones and therefore might be a generic property of focal onset seizures. We suggested that the hypercorrelated EEG activity, which consistently started to build up at the beginning of the second half of the seizures, could be an emergent self-regulatory mechanism to terminate seizure activity by driving extended neuronal networks simultaneously into a refractory state. Based on these data, however, we cannot definitely decide whether the increase of synchronization is causally related to seizure termination. Increasing

* Corresponding author. Tel.: +49 228 2871 5864; fax: +49 228 2871 6294.

E-mail address: kaspar.schindler@gmail.com (K. Schindler).

synchronization and seizure termination might still be concurrently related to an unidentified third phenomenon.

In favour of a causal role of increasing synchronization for seizure termination are the results of an extensive set of *in vivo* cat experiments with multi-site intracellular and extracellular as well as local cortical field potential recordings by Steriade and colleagues (summarized in Timofeev and Steriade, 2004). The authors investigated initiation, development, and cessation of seizures. In the initial stage of seizures they observed time-lags between cortical recordings of up to 150 ms, but the degree of synchrony progressively increased towards the late seizure stage (Topolnik et al., 2003). When all the affected neurons were drawn into highly synchronous paroxysmal activity, the seizures stopped. As an electrophysiological mechanism underlying seizure termination, it was proposed that Na^+ - and Ca^{2+} -activated potassium currents overcome hyperpolarization-activated depolarizing ionic currents. Importantly, this hypothesis is consistent with the experimental findings that – at the cellular level – seizure termination coincides with neuronal hyperpolarization, whereas hypoxic and hypercapnic conditions – that would result from rapid utilization of available metabolic substrates – cause neuronal depolarization (Caspers and Speckmann, 1972). Thus, seizure termination seems to be due to active processes that drive neurons into a refractory, hyperpolarized state and not simply result from metabolic depletion. One reason, why energy supply may not be a critical factor for seizure termination, is the significant increase of blood flow in epileptogenic cortex during seizures. This increase in blood flow is such a persistent and pronounced phenomenon that it is clinically used to reliably detect the seizure onset zones and propagation pathways by single photon emission computed tomography (Van Paesschen et al., 2007).

The goal of the present study was to find further evidence that hypersynchronized neuronal activity may be a mechanism to terminate seizures. To this end we analysed EEG recordings of status epilepticus. Status epilepticus may be defined as non-terminating seizure activity characterized by epileptiform EEG patterns and concurrent behavioural changes. Status epilepticus is further specified as “impending” if seizure activity lasts longer than 5 min and as “established” if seizure activity continues for more than 30 min (Chen and Wasterlain, 2006).

We specifically tested the following two hypotheses.

1. If increasing synchronization of neuronal activity is an important mechanism to terminate seizures, then there should not be strong and persistent hypersynchronization during status epilepticus, i.e., status epilepticus could be characterized by relatively impaired synchronization.
2. Some anticonvulsant drugs used to stop status epilepticus could work by enhancing synchronization. Thus, increasing synchronization should be observable after application of the anticonvulsant drug but before status termination.

2. Methods

2.1. EEG recordings

EEG signals were recorded either intracranially with strip-, grid-, and depth electrodes (all manufactured by AD-TECH, Wisconsin, USA) or with surface electrodes. Using a Stellate Harmonie recording system (Stellate, Montreal, Canada; amplifiers constructed by Schwarzer GmbH, München, Germany) EEG signals were sampled at 200 Hz, band-pass filtered either between 0.1 and 70 Hz (intracranial recordings) or between 0.1 and 25 Hz (extracranial recordings) and A/D converted at 16 bit resolution. With referential montage there would be a considerable risk that the reference electrode would record propagating seizure activity and could cause an artificial increase of correlation in the EEG recordings. Therefore only bipolar derivations between nearest neighbour electrode contacts were used. The terms “channel” and “bipolar derivation” are used synonymously here. For square grid electrodes only the bipolar derivations along one dimension (perpendicular to the attachment points of the connecting wires) were used. For extracranial recordings the channels containing the Fp1/Fp2 electrodes were excluded to minimize eye movement artifacts.

2.2. Synchronization analysis: the eigenvalue spectrum of the equal-time correlation matrix

2.2.1. The two-dimensional case

To assess the spatio-temporal evolution of synchronized neuronal activity we apply a method recently introduced to the field of EEG analysis by Müller et al. (2005). In this section we introduce basic concepts and illustrate characteristic aspects of this method for the simplest possible case of a short EEG signal consisting of only two channels $x(t)$ and $y(t)$ (Fig. 1a–d). In the next section we will then demonstrate, how the method can be extended to long-time recordings with many channels. To detect the presence of synchronized activity one may display the EEG as a scatter plot x versus y (Fig. 1a–d). At each time instant a single point represents the momentary EEG amplitudes of the two channels in the plane spanned by x and y . Displaying the complete 2.5 s of EEG shown in Fig. 1a, which was sampled at 200 Hz, results in the cloud of 500 points plotted in Fig. 1b. This cloud approximates an ellipse with major axis pointing from the lower left to the upper right of the x – y -plane. The shape and orientation of the cloud of points is due to the fact that large (small) values of x tend to occur together with large (small) values of y , i.e., the neuronal activity recorded in the two EEG channels is slightly synchronized. The directions of the major and minor axes of the ellipse approximated by the cloud of points are indicated by the red and blue arrows in Fig. 1b. These two arrows correspond to the so-called eigenvectors of the correlation matrix C , which is shown numerically in Fig. 1c. The elements of C are the pair-wise

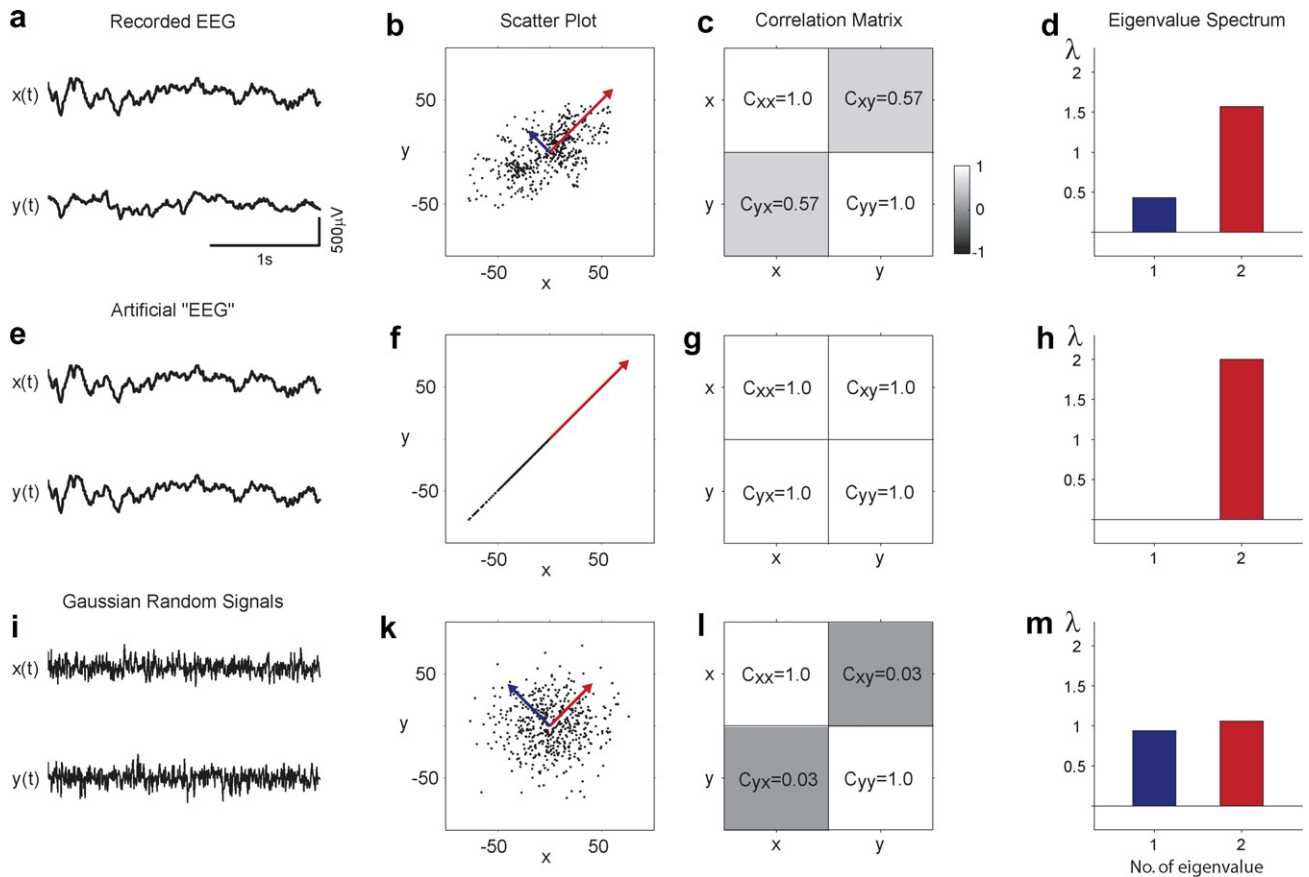


Fig. 1. Assessing synchronization by the eigenvalue spectrum of the zero-lag correlation matrix. (a) An EEG recording consisting of two channels $x(t)$ and $y(t)$, duration = 2.5 s, sampling rate = 200 Hz. (b) Plotting $x(t)$ versus $y(t)$ for each time point yields a cloud of 500 points, which approximates an ellipse. The two main axes of this ellipse are indicated by the red and the blue arrows. Size and direction of these axes correspond to the eigenvalues and eigenvectors of the zero-lag correlation matrix shown in (c). The eigenvalue spectrum is displayed in (d) and consists of the ordered eigenvalues $\lambda_1 \leq \lambda_2$. (e) Same analysis for an artificially created “EEG” signal that is perfectly synchronized ($x(t) = y(t)$). (f) In this case the points of the scatter plot form a line, the zero-lag cross correlation coefficients are all equal to 1 (g), and the eigenvalue spectrum degenerates to a single eigenvalue $\lambda_2 > 0$ (h). For two Gaussian random signals (i), the scatter plot approximates a circular shape (k), the off-diagonal elements C_{xy} and C_{yx} are close to zero (l) and the eigenvalues are both close to 1 (m). Synchronization is reflected in the structure of the eigenvalue spectra. For example desynchronization (as an example consider the transition from (h) to (m)) is accompanied by a decrease of λ_2 and an increase of λ_1 . (For interpretation of the references in colour in this figure legend, the reader is referred to the web version of this article.)

linear equal-time (=zero-lag) correlation coefficients defined as $C_{xy} = \frac{1}{L} \sum_{t \in L} \tilde{x}(t) \cdot \tilde{y}(t)$, where L denotes the duration of the signals in sampling points (=500 in the case of signals x and y) and the tilde sign indicates that $x(t)$ and $y(t)$ are normalized to zero mean and unit variance. C_{xy} varies from +1, if $x(t)$ and $y(t)$ are perfectly correlated to -1 , if $x(t)$ and $y(t)$ are exactly anticorrelated. If $x(t)$ and $y(t)$ are completely uncorrelated C_{xy} equals 0. Though the matrix C shown in Fig. 1c has only size 2×2 it illustrates two important properties, which apply to any larger $n \times n$ equal-time correlation matrix, too. Firstly, the elements C_{xx} and C_{yy} , which form the main diagonal running from the top left to the bottom right, equal one, reflecting that any signal is always perfectly correlated with itself. Secondly, due to the commutative property of linear equal-time correlation the elements C_{xy} and C_{yx} are identical. To generalize, the main diagonal of any equal-time correlation matrix consists of ones and any correlation matrix is symmetrical relative to its main diagonal.

According to fundamental results of linear algebra (Jolliffe, 2002), such a matrix C yields n real eigenvalues λ , which are found by solving $Cv_i = \lambda_i v_i$, where λ_i and v_i denote the eigenvalues and their associated eigenvectors. If the eigenvalues are sorted, for example in ascending order $\lambda_1 \leq \lambda_2 \leq \lambda_3 \leq \dots \leq \lambda_{\max}$, they form the spectrum of the correlation matrix C as illustrated in Fig. 1d. An eigenvalue λ_i indicates how strongly the signals are correlated in the direction of its corresponding eigenvector v_i . Therefore the larger eigenvalue λ_2 , represented by the red bar in Fig. 1d, is associated with the red eigenvector pointing in the direction of the major axis of the ellipse approximated by the cloud of points shown in Fig. 1b. Furthermore, the sum of the eigenvalues is always identical to the sum of the elements of the main diagonal of C , i.e., equal to $n = 2$ in the exemplary case (the sum of elements of the main diagonal is also called the “trace” of the matrix). Therefore, when one eigenvalue increases, at least one other has to decrease to keep the sum constant. This compensatory

decrease is sometimes, especially in nuclear physics, referred to as “level repulsion”. The crucial point here is that the eigenvalue spectrum is directly related to the synchronization of the EEG signal. To further clarify this essential characteristic of the analysis method consider the case of two perfectly synchronized EEG channels displayed in Fig. 1e. This is an artificial “EEG” created by copying the data of channel x to channel y . When plotting x versus y all the points now fall on the straight line that bisects the x – y -plane at an angle of 45° (Fig. 1f). All the bivariate correlation coefficients equal one (Fig. 1g), because the two channels are completely synchronized not only with itself, but by construction also with each other. The eigenvalue spectrum (Fig. 1h) has then only one eigenvalue $\lambda_2 > 0$, i.e., $\lambda_2 = 2$ and $\lambda_1 = 0$. Note that $\lambda_1 + \lambda_2 = 2 = \text{trace}(C)$ as requested. Another informative example is the case of two random Gaussian signals displayed in Fig. 1i. The scatter plot x versus y approximates a circular shape in the x – y -plane, indicating that there is only a minimal amount of random correlation, which is due to the finite duration of the signals. C_{xy} and $C_{yx} \approx 0$ and the two eigenvalues $\lambda_{1,2} \approx 1$. The eigenvalue spectrum of an EEG (Fig. 1d) lies between these two extreme cases of eigenvalue spectra for signals that are perfectly correlated (Fig. 1h) or completely uncorrelated (Fig. 1m). Note that the transition from two perfectly correlated to two completely uncorrelated signals will be reflected in the eigenvalue spectrum by a relative decrease of λ_2 and a relative increase of λ_1 .

2.2.2. The multi-dimensional case

A powerful aspect of using the eigenvalue spectrum of the equal-time correlation matrix to assess EEG synchronization is that the approach can easily be extended from the simple exemplary case of a short recording with only two channels to long-time recordings with many channels. This is illustrated in Fig. 2 for an EEG recorded with two hippocampal depth electrodes DL and DR with nine bipolar derivations each. The anatomical positions of DL and DR are shown in Fig. 2b. To account for the non-stationarity of the EEG, a short window w of duration 500 sampling points (2.5 s) is shifted along the recording in steps of $\Delta t = 100$ sampling points (0.5 s). The cloud of points representing the EEG recording in a scatter plot now extends in an 18-dimensional space and therefore cannot be directly visualized any more as it was possible for the two-dimensional case before (Fig. 1). However, the correlation matrix C may still be plotted as shown in Fig. 2c. Note the properties of C that are already familiar from the two-dimensional case discussed before, namely that the elements of the main diagonal are all equal to 1 and that C is symmetrical relative to its main diagonal. In the next step, the eigenvalue spectrum is computed (Fig. 2d). The eigenvalues are then arranged as the column of a new matrix (shown in white) and associated with the time of the beginning of w . Then w is shifted forward in time by Δt and the procedure is repeated. The changes of the eigen-

value spectra over time are difficult to recognize in the three-dimensional bar chart displayed in Fig. 2e and two additional steps of post-processing are applied. First, the data are represented by a two-dimensional colour-coded map, which corresponds to looking at the three-dimensional bar chart from directly above, and encoding the heights of the bars by different colours. However, because there are large absolute differences between the eigenvalues at the upper end and those of the rest of the spectrum, the relative changes of the smaller eigenvalues over time are still not visible. Therefore, each eigenvalue is normalized by first subtracting its temporal average and then dividing by its standard deviation over time. This yields the representation shown in Fig. 2g, where the relative changes of the eigenvalue spectrum are now clearly visible. Increases of synchronization are reflected by a relative increase of the eigenvalues at the upper end of the spectrum and a relative compensatory decrease of the eigenvalues of the rest of the spectrum. Correspondingly, desynchronization of neuronal activity causes a relative increase of the lower eigenvalues and a compensatory decrease of the larger eigenvalues. It is important to realize that due to the large absolute differences between the eigenvalues at the upper and those at the lower end of the spectrum, a small non-significant absolute change of some large eigenvalue may cause a large and statistically significant relative change of one or of a group of small eigenvalues. Therefore, the lower end of the spectrum is not just representing “noise” but provides important information that might be lost if the analysis were restricted to the large eigenvalues only (Müller et al., 2005), as is for example done in classical principal component analysis, where the main goal is “data reduction” (Jolliffe, 2002). Nevertheless, even computing the complete eigenvalue spectrum consisting of n eigenvalues still provides a very efficient way of representing the correlation structure implicit in a $n \times n$ correlation matrix with $\frac{n(n-1)}{2}$ different correlation coefficients.

2.2.3. Generic dynamics of eigenvalue spectrum during focal-onset seizures

The typical result of applying the method to a 79 channel EEG recording of a seizure with focal onset is shown in Fig. 3. The seizure started with low-amplitude high-frequency activity in the left occipital lobe (OL 5–6), which is, however, not clearly discernable at the large scale of resolution used to depict the complete peri-ictal EEG including several minutes of postictal recording (Fig. 3a). In Fig. 3c the relative changes of the eigenvalue spectrum are plotted. The example clearly demonstrates how the neuronal activity first decorrelates, indicated by a relative decrease of the few largest eigenvalues and a compensatory broad-banded relative increase of the smaller eigenvalues. Then EEG activity starts to resynchronize around time ~ 2 min, well before the seizure terminates. Note how epileptiform activity stops in most EEG channels simultaneously, which is a further evidence that synchronized neuronal activity may be important for seizure termina-

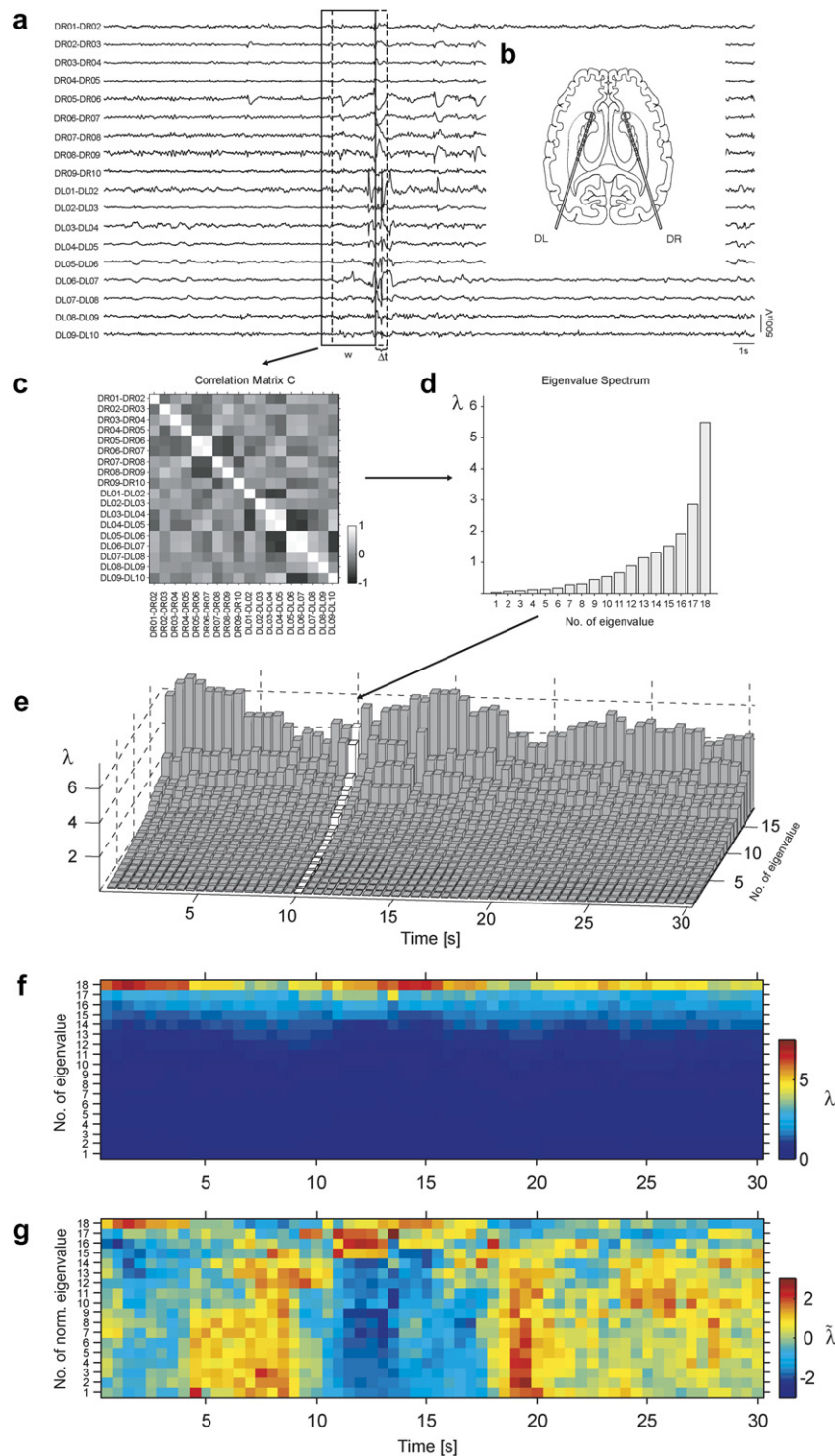


Fig. 2. Assessing and visualizing the changes of EEG synchronization. (a) The 18-channel EEG inside a sliding window of length $w = 2.5$ s (500 sampling points) is normalized channel-wise to zero mean and unit variance (not shown) before the zero-lag correlation matrix displayed in (c) is computed. The 18×18 correlation matrix is symmetrical relative to the main diagonal and therefore has 18 eigenvalues ≥ 0 . Sorting the eigenvalues in an ascending order $\lambda_1 \leq \lambda_2 \leq \lambda_3 \dots \leq \lambda_{18}$ gives the eigenvalue spectrum (d), which is associated with the first time point of the sliding window and arranged as the column of a new matrix shown (in white) in (e). The sliding window is then moved forward in time by Δt and the steps illustrated in (c–e) are repeated. The relative changes of the eigenvalues over time are almost impossible to see in a three-dimensional representation such as in (e). Therefore two post-processing steps are applied. First, the eigenvalues are represented as a colour-coded two-dimensional plot (f) and each eigenvalue is normalized by first subtracting its temporal average and then dividing by its standard deviation over time. Now the relative changes of the normalized eigenvalues $\tilde{\lambda}_i$, where i runs over all 18 channels, are clearly visible in (g). The EEG used was recorded by two depth electrodes DL and DR with anatomical positions as shown in (b).

tion. The postictal state is then characterized by a relative hypersynchronization as is reflected by the largest eigenvalues staying elevated and the remaining smaller eigenvalues decreased. The relative hypersynchronization persists for several minutes before it slowly starts to loosen. An even more compact visualization of synchronization dynamics is achieved when the time courses of the averages

of the five largest and the 50 smallest normalized eigenvalues are displayed as shown in Fig. 3d. This plot clearly shows the level repulsion phenomenon, i.e., the reversed behaviour of $\bar{\lambda}_{\text{mean}}^{75:79}$ and of $\bar{\lambda}_{\text{mean}}^{1:50}$. It furthermore demonstrates that the relative changes of the smaller eigenvalues may be more pronounced than the relative changes of the larger eigenvalues. This evolution of synchronization as

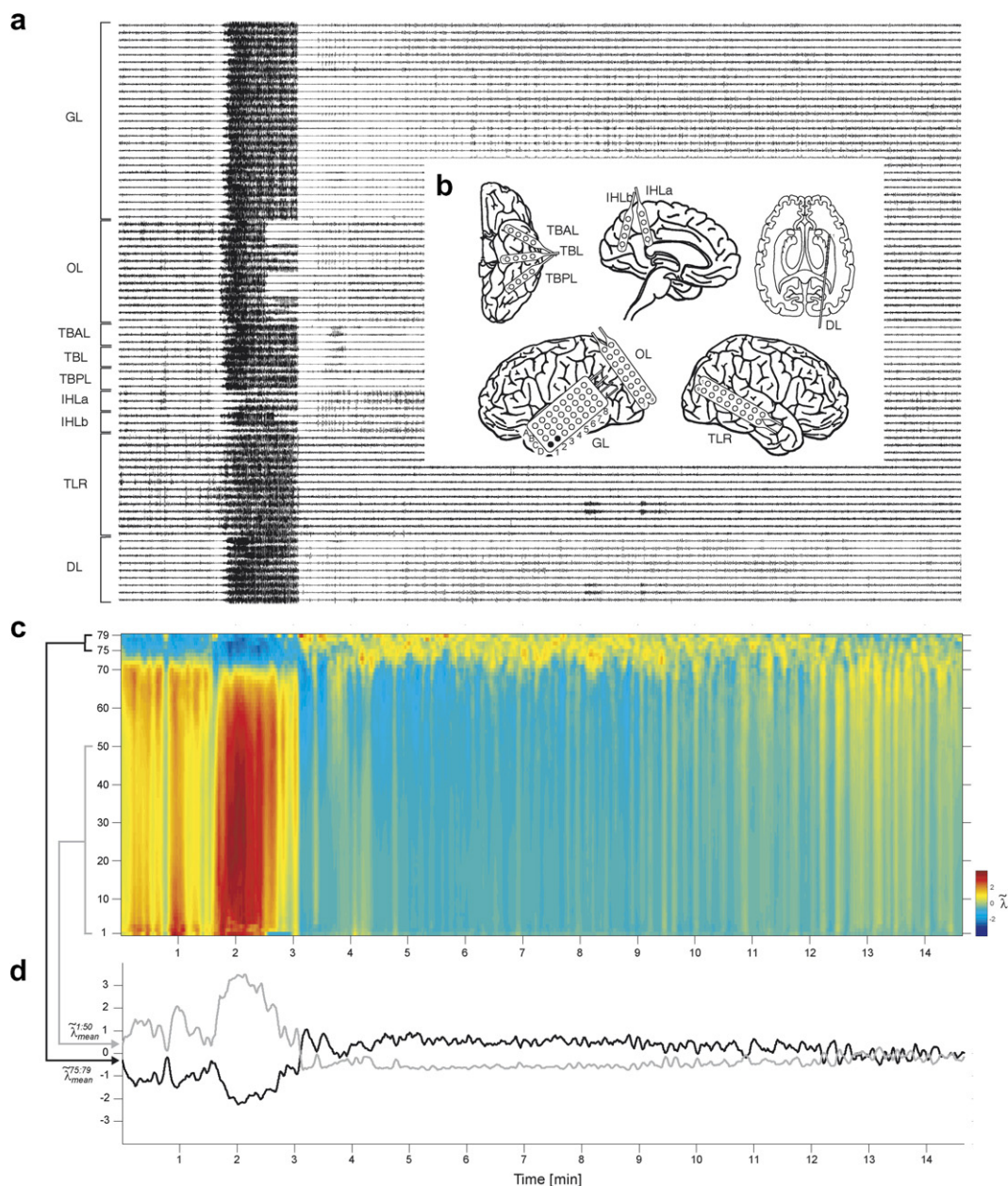


Fig. 3. The generic evolution of peri-ictal synchronization for an epileptic seizure with focal onset. Semiology was consistent with temporal lobe seizures, but surface EEG also displayed occipital epileptiform activity. Intracranially recorded EEG and anatomical positions of electrodes are displayed in (a and b). Channels GLD1-2 (marked by filled black circles on the grid in (b)) were persistently contaminated by artifacts and were therefore excluded from analysis. The EEG onset pattern in OL 5–6 is not discernible at this relatively large scale. The relative changes of all eigenvalues are shown in (c), smoothed by a moving average filter with a window length of 5 s. During the initial stages of the seizure, EEG activity desynchronizes as indicated by a relative decrease of the larger eigenvalues and a strong relative increase of the smaller eigenvalues. Resynchronization starts after time = 2 min, clearly before the seizure terminates. In (d) the average of the five largest ($\bar{\lambda}_{\text{mean}}^{75:79}$) and the 50 smallest normalized eigenvalues ($\bar{\lambda}_{\text{mean}}^{1:50}$) is plotted, demonstrating that the relative changes of the smaller eigenvalues are even more pronounced than the changes of larger eigenvalues. The relatively increased synchronization persists into the postictal period and only gradually loosens.

assessed by the changing correlation structure was found to be generic of focal onset seizures in a recent study (Schindler et al., 2007). In addition to illustrating how the analysis method works, the typical results for a single seizure may serve here as a comparison to the results of analysing EEGs recorded during status epilepticus described below.

3. Results

Our electronic video-EEG database of the years 2001–2005 was searched for recordings of status epilepticus that included termination of epileptiform activity and contained minimal or no artifacts. Six recordings, one of an impending and five of an established status epilepticus, from six patients met these criteria and were included in the present study. Clinical information about the six patients is summarized in Table 1. EEGs of patients #1 and #2 were recorded with intracranial, those of patients #3 to #6 with surface electrodes.

Patient #1 suffered from perinatal brain injury with subsequent symptomatic pharmaco-resistant epilepsy. Previous investigations had led to complete callosotomy in 2004, because most of her seizures were epileptic drop attacks. Her seizure rate did not decrease significantly, but after callosotomy seizure onsets could be lateralized to her left hemisphere. Therefore she underwent pre-surgical evaluation with intracranial electrodes positioned as depicted in Fig. 4b. Cortical representation of language was localized by assessing if focal electrical stimulation (trains of bipolar symmetrical current pulses at 30 Hz and with amplitudes ranging from 1 to 4 mA) interfered with performance during neuropsychological language tasks. During such a cortical mapping procedure, a prolonged epileptic seizure of more than 10 min duration and therefore fulfilling the definition of impending status

epilepticus was triggered as displayed in Fig. 4a. The relative changes of the eigenvalue spectrum, i.e., the time courses of $\hat{\lambda}$, are plotted in Fig. 4c. In addition, the more compact representation using averages of largest and smallest eigenvalues is shown in Fig. 4d. These two graphs clearly illustrate that EEG synchronization stays unchanged for approximately the first 2 min of the seizure and only then starts to slowly increase as reflected by a relative increase of the larger eigenvalues and a compensatory relative decrease of the smaller eigenvalues. This process of increasing synchronization is reversed around time ~ 7 min, when epileptiform activity spreads further and causes clinically secondary generalization. From ~ 7 to 9.5 min EEG desynchronizes as reflected by an increase of the smaller and a decrease of the larger eigenvalues. Resynchronization then starts at ~ 9.5 min and becomes progressively stronger, reaching its maximum when the impending status epilepticus terminates spontaneously. In Fig. 5 the EEG around termination of the impending status epilepticus is plotted on a time scale normally used for clinical visual analysis together with the time-aligned averages of the largest and of the smallest eigenvalues. This recording supports our first hypothesis, that neuronal synchronization as recorded by EEG during ongoing status epilepticus is relatively impaired and does not become strong enough to stop epileptiform activity.

Patient #2 had pharmaco-resistant temporal lobe epilepsy with frequent complex-partial and rare secondarily generalized seizures. MR imaging revealed left-sided atrophy and hyperintensity in T2-weighted sequences of the hippocampal structures consistent with hippocampal sclerosis (HS). However, in addition there was atrophy and slight blurring of the borders between white and gray matter of the left lateral temporal lobe. Therefore intracranial EEG recording was performed to rule out seizure onsets in

Table 1
Clinical information

Patient	Gender/ age ^a [y]	Epilepsy duration [y]	Clinical history	Seizure type ^b	Clinical neurological exam	MR findings	Surgical outcome ^c
#1	f/33	10	Perinatal left hemispheric damage, callosotomy 2004	SP(DA)/CP/sGTC	Right sensomotor hemisindrome	Complete callosotomy, enlarged left lateral ventricle	No surgery
#2	f/44	43	Inconspicuous	CP/sGTC	No focal deficits	Left HS, slight atrophy of left anterior and lateral temporal lobe	sAHE, IC
#3	m/17	12	Progressive myoclonus epilepsy	GTC	Unconscious, brainstem reflexes intact, intermittent myoclonia	Diffuse subcortical hyperintensities	No surgery
#4	m/80	1	Limbic encephalitis, acute pneumonia	CP/sGTC	Fluctuating vigilance, no focal deficits	Bilateral hippocampal atrophy	No surgery
#5	f/42	30	Inconspicuous	sGTC	No focal deficits	Normal	No surgery
#6	f/48	20	Childhood febrile seizures	CP/sGTC	No focal deficits	Left HS	sAHE, IA

^a Age when status epilepticus was recorded.

^b SP, simple partial; DA, drop attacks; sGTC, secondarily generalized tonic-clonic; CP, complex partial.

^c sAHE, selective amygdalo-hippocampectomy, IC/IA according to Engel et al. (1993).

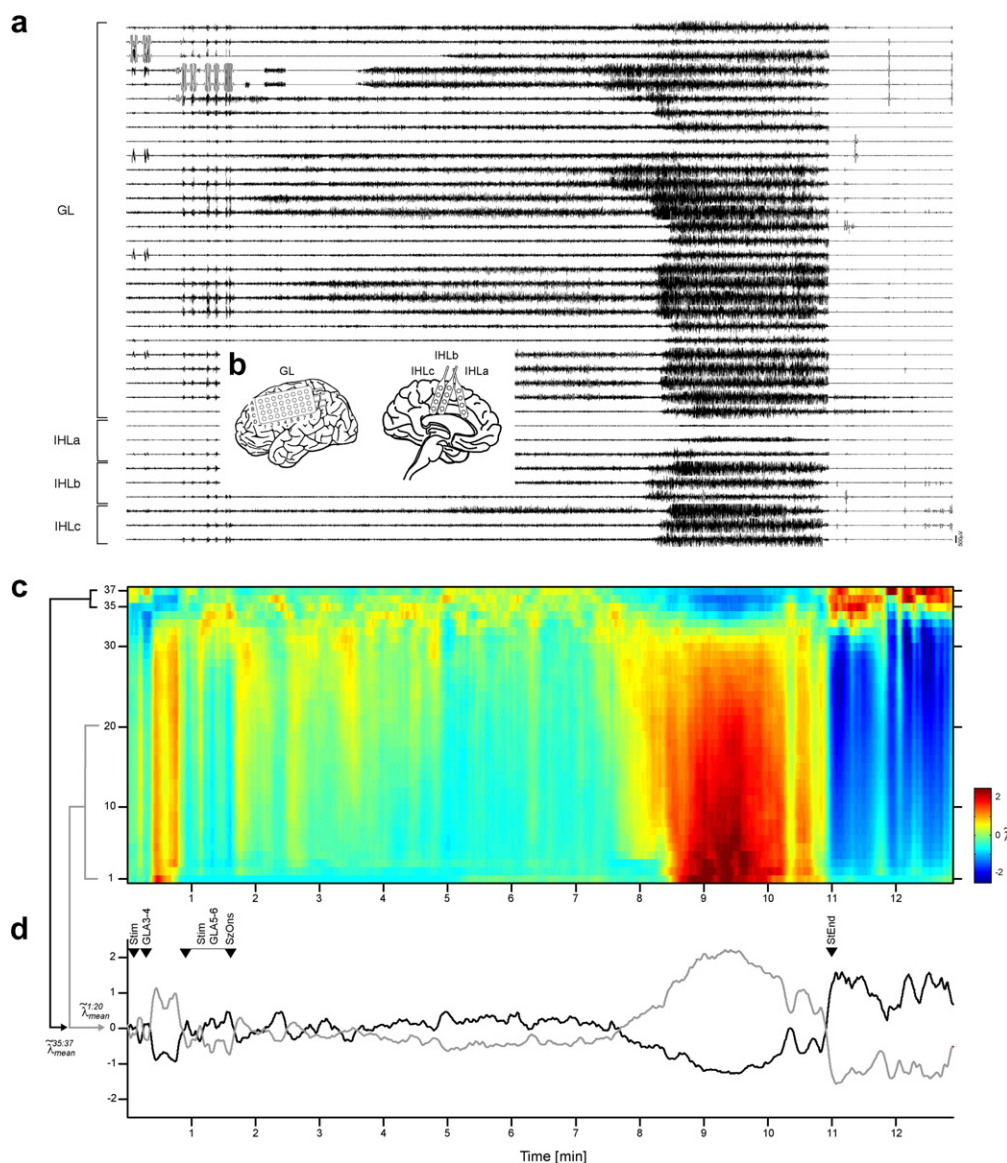


Fig. 4. Impending status epilepticus of patient #1 triggered by focal electrical brain stimulation used for cortical language mapping. Intracranially recorded EEG and anatomical positions of electrodes are shown in (a and b). The changing eigenvalue spectrum, which has been smoothed by a moving average with a window length of 5 s, is displayed in (c), with the more compact representation of $\tilde{\lambda}_{\text{mean}}^{35:37}$ and $\tilde{\lambda}_{\text{mean}}^{1:20}$ in (d). The seizure is triggered by stimulating grid contacts GLA4–5. During ongoing seizure activity, synchronization is relatively low and increases only slightly. Secondary generalization is first accompanied by strong desynchronization. Resynchronization starts around 9.5 min and reaches its highest level when the impending status epilepticus terminates. Abbreviations: Stim, stimulation; SzOns, seizure onset; StEnd, spontaneous termination of impending status epilepticus.

the left lateral temporal region. Despite careful and slow reduction of her anticonvulsant medication, the patient suffered from status epilepticus, which lasted more than 4 h and stopped after the application of several anticonvulsive drugs. In Fig. 6a, selected parts of her EEG are displayed, with the anatomical positions of the intracranial electrodes shown in Fig. 6b. The complete time course of the relative changes of the eigenvalue spectrum is plotted in Fig. 6c, the relative changes of the average of the five largest eigenvalues $\tilde{\lambda}_{\text{mean}}^{42:46}$ and of the 30 smallest eigenvalues $\tilde{\lambda}_{\text{mean}}^{1:30}$ in Fig. 6d. The status epilepticus started with a complex-partial seizure with a semiology typical for the patient. The seizure began in the left hippocampus, as can be seen

from the continuous epileptiform activity emerging in the posterior channels of the depth electrode DL (left-most panel of Fig. 6a). During the seizure EEG first desynchronized as indicated by the typical pattern of increasing small and decreasing larger eigenvalues. Note that also in this case the relative increase of $\tilde{\lambda}_{\text{mean}}^{1:30}$ is more pronounced than the decrease of $\tilde{\lambda}_{\text{mean}}^{42:46}$. Desynchronization was followed by a slight but transient increase of synchronization after the first application of lorazepam (1 mg), but epileptiform activity did not terminate. Despite the repeated application of lorazepam, first impending and then established status epilepticus developed. Approximately 55 min after onset there was secondary tonic-clonic generalization. Secondary

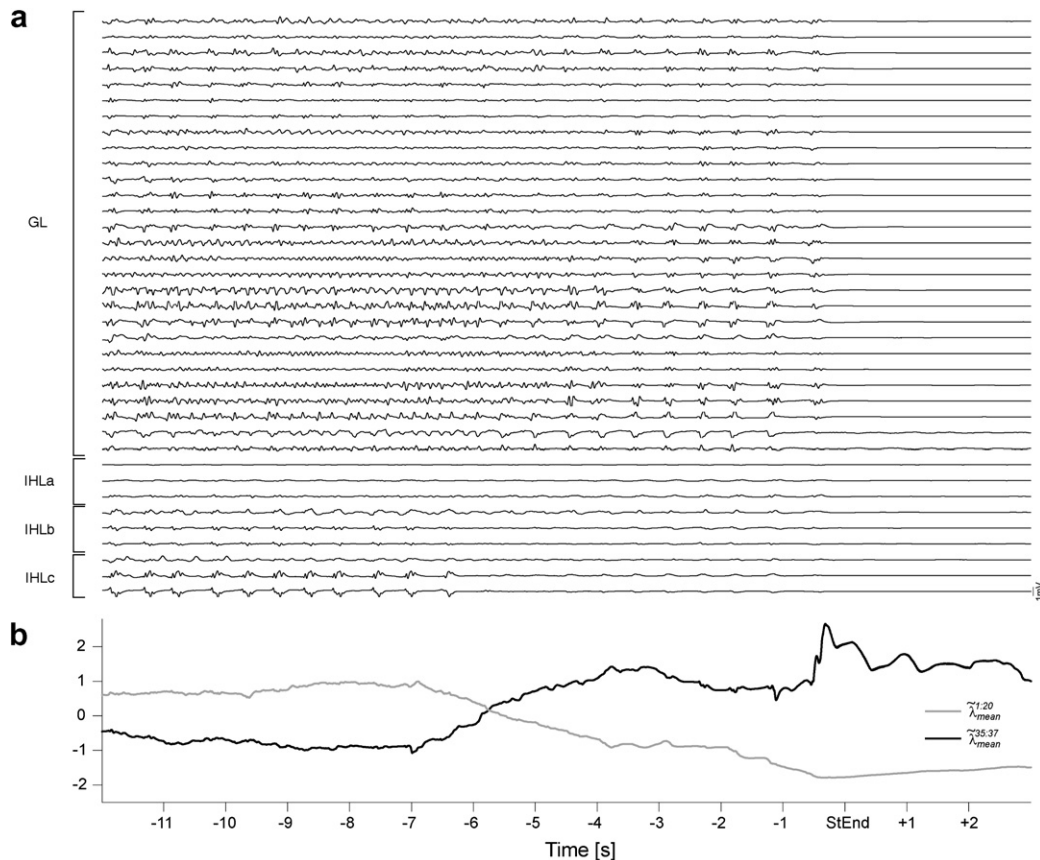


Fig. 5. Spontaneous termination of impending status epilepticus of patient #1 displayed with higher temporal resolution. The bipolar EEG is plotted in (a), showing generalized rhythmic patterns slowing down towards the spontaneous end of the impending status (StEnd). Approximately 7 s before StEnd, EEG synchronization begins to further increase as indicated by the increase of $\tilde{\lambda}_{\text{mean}}^{35.37}$ and the decrease of $\tilde{\lambda}_{\text{mean}}^{1.20}$ plotted in (b). Six seconds before StEnd, sharp waves disappear in IHLc. EEG rhythms further slow down, and at StEnd, rhythmic EEG patterns cease simultaneously in all channels.

generalization ended with transiently increased synchronization of neuronal activity (Fig. 6c and d), but continuous epileptiform discharges persisted in a subset of EEG channels as displayed in the second panel of Fig. 6a. For the next 2 h levels of EEG synchronization fluctuated with a bias towards slight desynchronization. The patient continued to be unresponsive and showed intermittent oral and manual automatisms, deambulatory behavior and transient twitching of her right-sided facial muscles. Intravenous application of 750 mg phenytoin had no observable effects on behaviour or EEG and therefore diazepam drop-lets were administered orally. Approximately 15–20 min later synchronization of neuronal activity started to increase and to remain persistently elevated (note that the two short drops of the level of synchronization were due to artifacts). Epileptiform activity first gradually loosened and then stopped completely. The final distributed blunt sharp waves are shown in the right-most panel of Fig. 6a. The changes of neuronal activity were also accompanied by clinical improvement of the patient. Muscular twitching stopped, automatisms terminated and she regained consciousness. This investigation supports our first as well as our second hypothesis. As in the first case of status epilep-

ticus analysed above, it demonstrates that continuous epileptiform activity is accompanied not by hyper-, but on the contrary rather desynchronized EEG signals. In addition, it further shows that certain anticonvulsant drugs may re-increase and sustain EEG synchronization, which is then followed by termination of ictal discharges.

EEGs of patients #3 to #6 were recorded with surface electrodes. Changes of EEG synchronization and their relationship to the application of anticonvulsant drugs and status termination are illustrated in Fig. 7. Note that Fig. 7a–c only document status endings. The higher variance of the signals displayed in Fig. 7 relative to those for example shown in Fig. 6d is due to the smaller number of electrodes and to the more pronounced muscle and movement artifacts typical for surface EEG recordings. Despite this larger variance it is clearly observable in Fig. 7a–c that hypersynchronization develops gradually after application of anticonvulsant drugs, indicated by a relative decrease of the smaller eigenvalues and an increase of the largest eigenvalue. This gradual increase of EEG synchronization was accompanied by fading and then vanishing of rhythmic ictal patterns as demonstrated for patient #4 in Fig. 8. In patients #4 to #6 the changes of

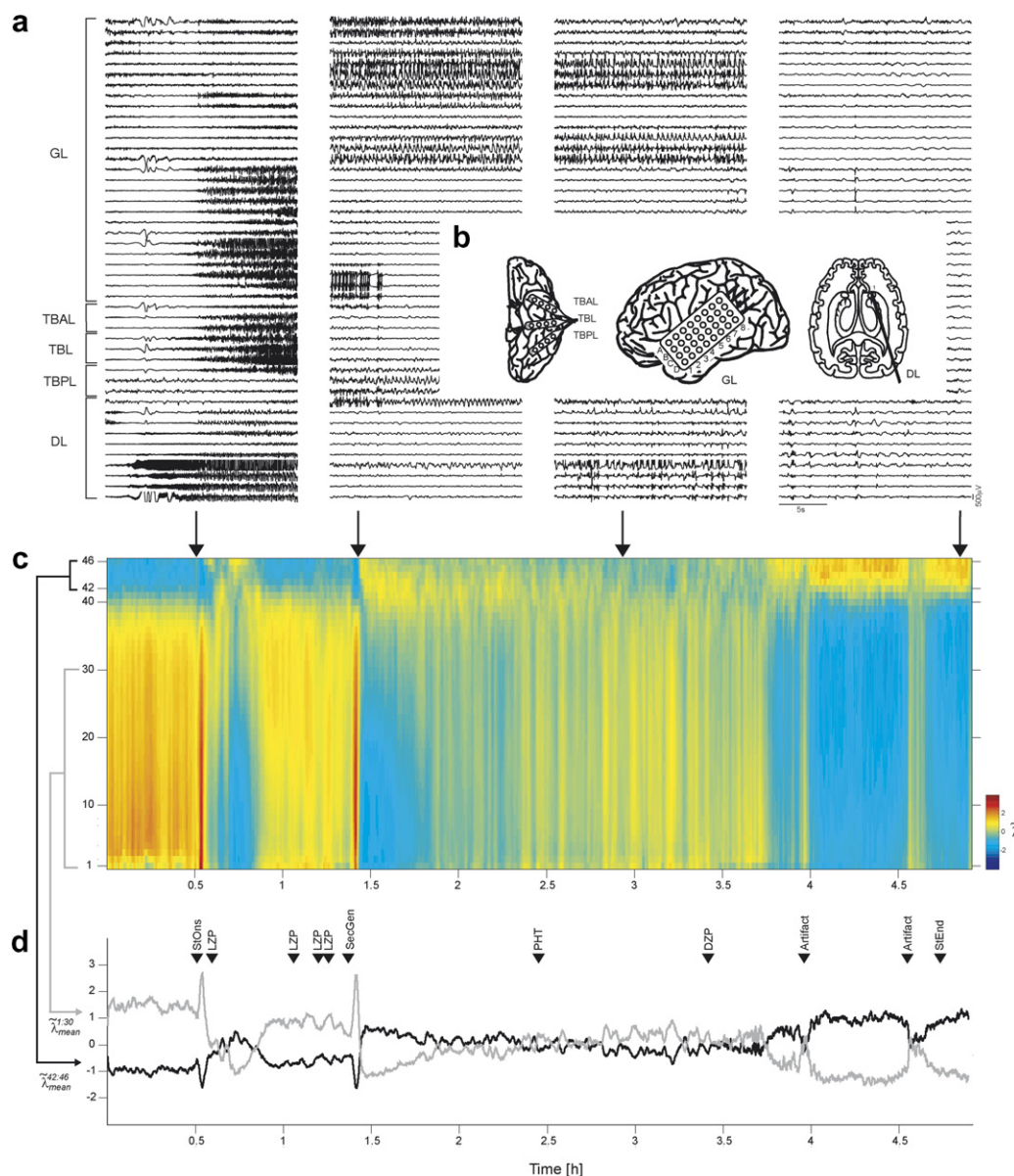


Fig. 6. EEG synchronization during status epilepticus in a patient with left temporal lobe epilepsy. Selected parts of the intracranially recorded EEG from the beginning, the end of the secondarily generalized episode, during ongoing status epilepticus and at the end of status epilepticus are displayed in (a). Anatomical positions of the electrodes are shown in (b). The full temporal course of the changes of the eigenvalue spectrum (smoothed by a moving average with a window length of 5 s) is plotted in (c) and the changes of $\lambda_{\text{mean}}^{42:46}$ and $\lambda_{\text{mean}}^{1:30}$ in (d). (For details see text.) Abbreviations (chronological order): StOns, status onset; LZP, lorazepam (1 mg tablet); SecGen, secondary generalization; PHT, phenytoin (750 mg intravenously); DZP, diazepam (droplets equivalent to 10 mg); StEnd, end of status.

EEG synchronization were accompanied by regaining consciousness, in patient #3 who suffered from progressive myoclonus epilepsy and who had been in prolonged coma, only the epileptiform activity stopped. Note that in patient #6 (Fig. 7d) the transition from desynchronized to hypersynchronized EEG activity occurred so rapidly that it did not clearly precede status termination (cf. Fig. 9).

4. Discussion

The aim of this study was to test whether increasing neuronal synchronization as reflected in increasing EEG

synchronization might be causally related to the termination of ictal activity. As the first testable hypothesis was proposed that if increasing neuronal synchronization was an important mechanism to stop epileptiform activity, then there should not be strong and persistent hypersynchronization during status epilepticus. Our results are consistent with this hypothesis, showing that synchronization fluctuates at only moderately elevated levels during prolonged seizure activity and only strongly and persistently re-increased before, or in one case (patient #6), when epileptiform discharges stopped. In our recent study (Schindler et al., 2007) we investigated only focal onset seizures

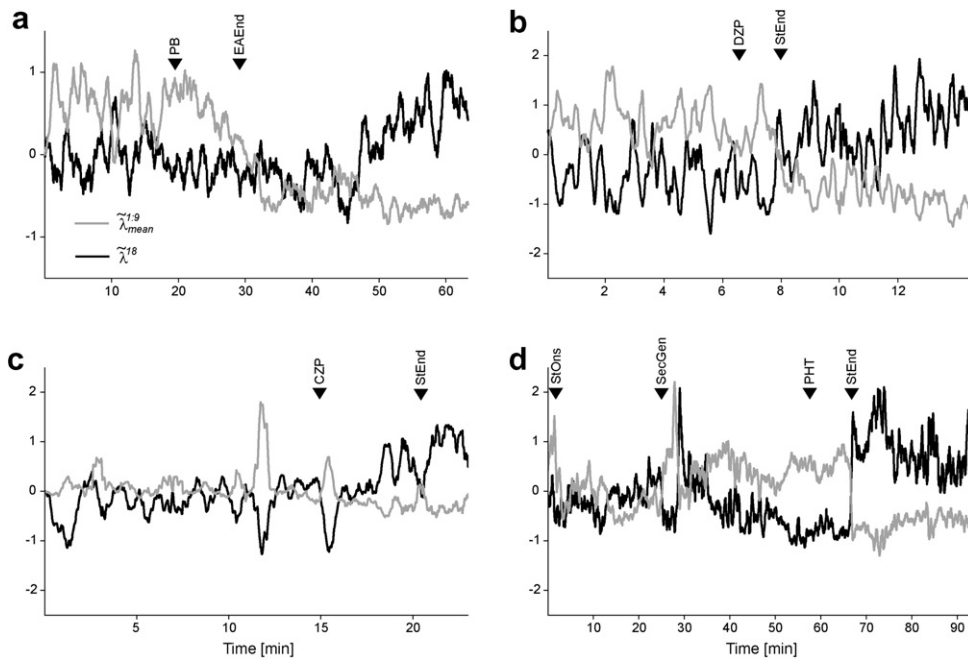


Fig. 7. Surface EEG synchronization of status epilepticus recordings from patients #3 to #6 as reflected by $\tilde{\lambda}^{18}$ and $\tilde{\lambda}_{\text{mean}}^{1-9}$. (For details see text.) Abbreviations: StOns, onset of status epilepticus; StEnd, end of status epilepticus; EAEnd, end of epileptiform activity (no clinical improvement); PB, Phenobarbital; DZP, diazepam; CZP, clobazam; PHT, phenytoin; SecGen, secondary generalization.

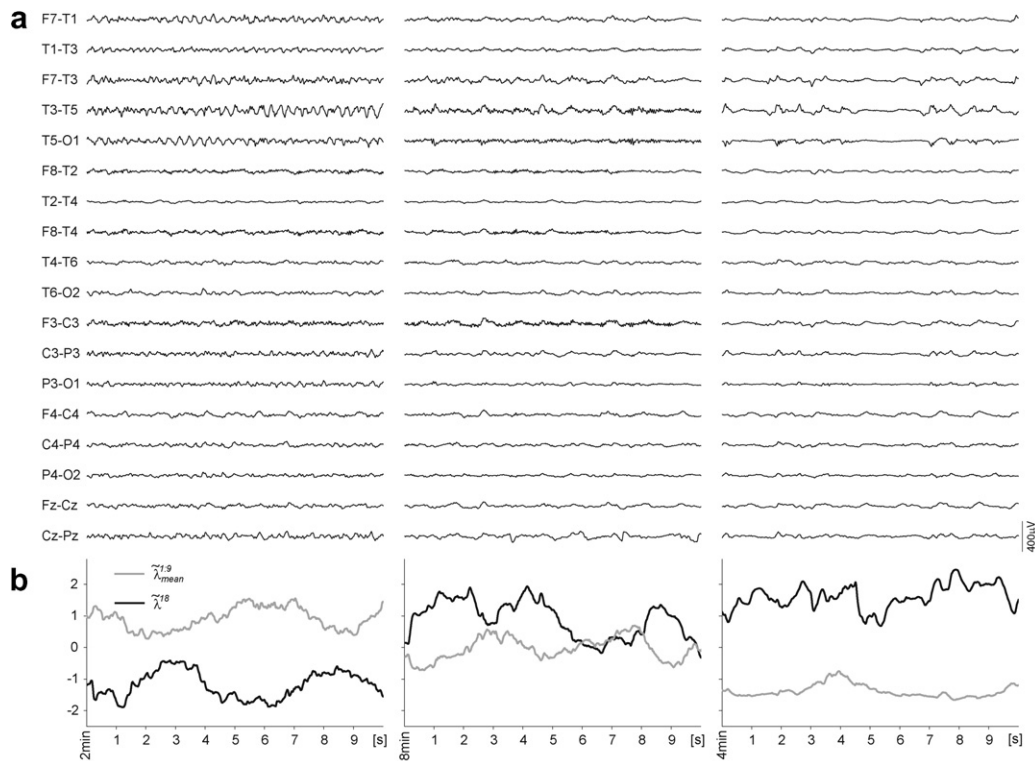


Fig. 8. Increase of EEG synchronization was accompanied by fading of rhythmic ictal patterns in patient #4. In (a), three 10 s time periods are displayed, beginning after 2, 8 and 14 min relative to the complete recording (compare Fig. 7b). (b) Time courses of the largest eigenvalue $\tilde{\lambda}^{18}$ and the average of the smallest eigenvalues $\tilde{\lambda}_{\text{mean}}^{1-9}$. The first EEG period shows rhythmic ictal delta–theta activity mainly over the left temporal region. The relatively high values of $\tilde{\lambda}_{\text{mean}}^{1-9}$ and low values of $\tilde{\lambda}^{18}$ indicate that this activity is desynchronized. During the second EEG period rhythmic temporal activity has further slowed down and lost amplitude and is about to vanish completely. $\tilde{\lambda}^{18}$ has increased, and $\tilde{\lambda}_{\text{mean}}^{1-9}$ has decreased, indicating an increase of EEG synchronization. The third EEG period reveals short groups of pleomorphic delta waves over the left temporal region. $\tilde{\lambda}^{18}$ has further increased, while $\tilde{\lambda}_{\text{mean}}^{1-9}$ has clearly decreased, indicating that the postictal EEG activity is relatively hypersynchronized. Note that this clear difference of synchronization may hardly be appreciated from visual inspection of the EEG signals.

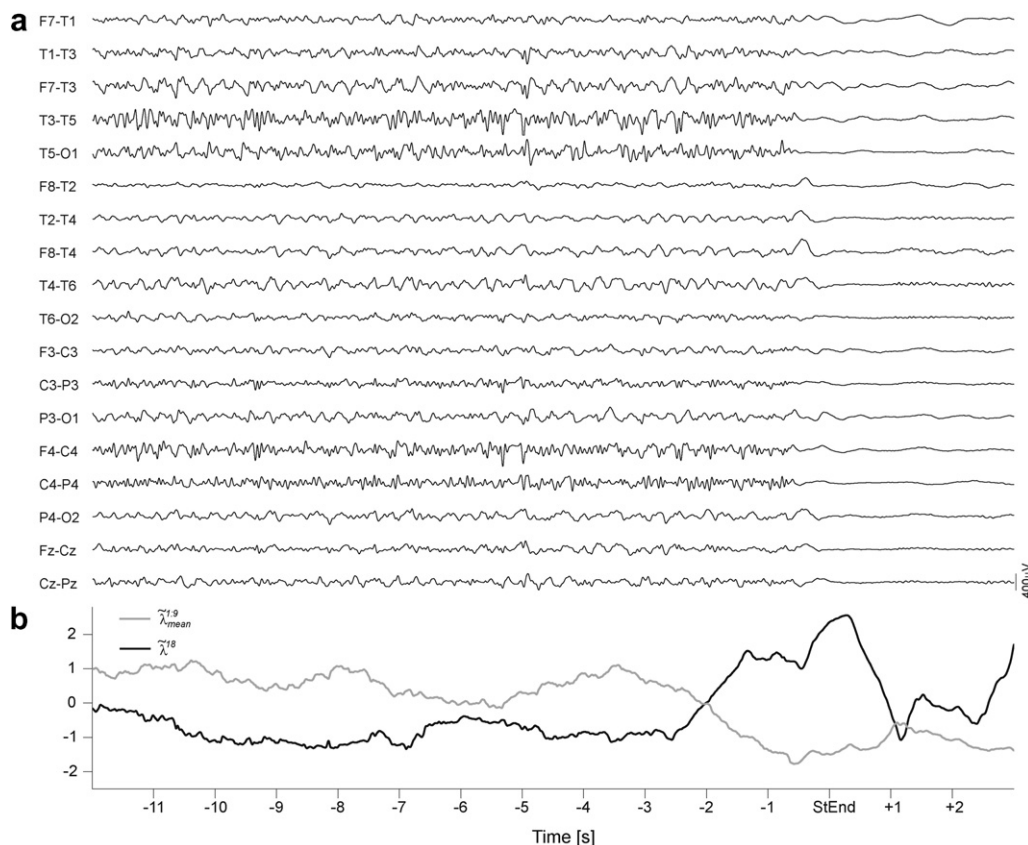


Fig. 9. Increase of EEG synchronization at status termination. EEG from patient #6 is displayed in (a), time courses of the largest eigenvalue $\bar{\lambda}^{18}$ and the average of the smallest eigenvalues $\bar{\lambda}_{\text{mean}}^{1-9}$ in (b). After intravenous application of phenytoin epileptiform activity simultaneously vanished in all EEG channels. Note that the increase of $\bar{\lambda}^{18}$ and the decrease of $\bar{\lambda}_{\text{mean}}^{1-9}$ that start 2.5 s before status termination are probably due to the inclusion of postictal EEG into the moving window used for synchronization analysis and must not be interpreted as an increase of EEG synchronization genuinely preceding status termination. StEnd, end of status epilepticus.

with an average duration of approximately 2 min. Based on these data we could not definitely decide whether increasing synchronization was causally related to seizure termination. If synchronization increased with continuing seizure activity then we should have measured very high synchronization levels during status epilepticus. However, we found a strong and persistent increase in synchronization only before or at the end of status epilepticus supporting an active role of synchronization in the termination of epileptiform discharges.

Our second hypothesis suggested that if increasing synchronization was an important mechanism to stop seizures, then some anticonvulsant drugs could work by enhancing synchronization. Thus, increased synchronization should occur after drug application, but precede seizure termination. We found this evolution of synchronization most clearly after the administration of diazepam (patients #2 and #4), clobazam (patient #5), the first time after lorazepam was given to patient #2 and after phenobarbital (patient #3). In patient #6 the change from relatively desynchronized to strongly synchronized EEG activity followed treatment with phenytoin but occurred so rapidly that it could not be temporally separated from seizure

termination. The numbers of recordings analysed for the different anticonvulsive drugs are small and therefore it is impossible to draw any strong conclusions about the mechanisms of action of these substances on the network level assessed by EEG. Nevertheless it is notable that diazepam, clobazam, lorazepam, and phenobarbital, which enhance GABAergic transmission, also increased EEG synchronization. This finding is in line with the important role GABAergic transmission plays in neuronal synchronization (Cobb et al., 1995; Bernard, 2005; Jedlicka and Backus, 2006). The sudden change to high synchronization after the application of phenytoin (Fig. 7d) might be due to the well-known non-linear pharmacokinetics of this drug, which may lead to accelerated increases of plasma levels despite a constant infusion rate (Hvidberg and Dam, 1976). Another possible explanation is that sodium channel blocking, which is considered to be the main anti-convulsive mechanism of phenytoin, does not lead to a gradual build up of neuronal synchronization detectable by EEG.

Reentrant spiral waves are considered a possible pathophysiological basis for cardiac tachyarrhythmias. The spread of these waves is then blocked and the waves are

annihilated by using a “defibrillator” (Glass and Josephson, 1995). This external device allows the application of electrical currents that create a spatially extended transiently refractory zone in the myocardium. The central nervous system and the heart do not of course have an identical anatomical structure. One of the most important differences is the existence of long-range connections in the brain. Despite the structural differences, however, both the brain and the heart share the important property that any pattern of activity may only propagate when there are elements that are not refractory. In cardiac emergencies a defibrillator is used to artificially create a refractory state of the myocardium that terminates the disordered spreading waves of excitation, which gave rise to the life-threatening arrhythmia. The results of our study further corroborate the idea that the brain may achieve a similar effect by self-organizing into a spatio-temporally extended transient state of refractoriness that blocks further spread of disordered (desynchronized) ictal activity. Thus, we propose that the ictal increase of synchronized neuronal activity as recorded by EEG may be considered an emergent self-regulatory mechanism for seizure termination. This hypothesis is also consistent with the typical evolution of seizure activity from high to low frequencies, because low-frequency oscillations need less precise synchronization to establish a simultaneously occurring refractory state. The hypothesis might furthermore explain why seizures often terminate simultaneously in spatially separated cortical regions (Fig. 3).

At this point of discussion it has to be stressed that we consider increased neuronal synchronization to be only one of several possible ways to terminate seizures.

A limitation of our study is the relatively low number of patients, which is due to the fact that acute status epilepticus is a life-threatening condition (Logroscino et al., 2005) and those patients are initially most often directly admitted to intensive care units and not to a specialized epilepsy clinic. Furthermore, during pre-surgical evaluations we of course try to prevent the occurrence of status epilepticus by reducing anticonvulsant medications very slowly. Therefore, EEG recordings of status epilepticus with intracranial electrodes are expected to, and actually should be, exceedingly rare. A limitation of our analysis method in its present form is that it is not frequency-selective, may not detect non-linear correlations, and does not take into account time-shifts. In addition, we cannot rule out, that other physiological mechanisms, besides neuronal synchronization, like local changes of excitability due to for example cerebral edema might affect the EEG correlation structure as assessed by the eigenvalue spectrum.

Despite these caveats, it is noteworthy that we found indications that different drugs may also have different effects on EEG synchronization. This implies that multivariate analysis methods might also be powerful extensions for pharmaco-EEG studies (Galderisi and Sannita, 2006). These methods may allow efficient screening of new substances for anticonvulsive effects that are due to changing

the collective synchronous activity of extended neuronal networks and that may be undetectable when only investigating the effects on the level of ion-channels or single neurons. In addition, it would be very interesting to assess how endogenous neurochemicals implicated in seizure termination, like e.g. adenosine, affect EEG synchronization (Young and Dragunow, 2006).

Electrical brain stimulation is a promising new therapeutic tool for patients suffering from pharmaco-resistant epilepsy (Osorio et al., 2005; Morrell, 2006). However, at present it is unclear, which are the optimal stimulation parameters to induce persistent anticonvulsant effects. On the assumption that epileptic seizures are due to hypersynchronous activity it has been speculated that electrical stimulation should be adjusted in a way to induce desynchronization (Milton and Jung, 2003). Our results indicate that the opposite may be the case, namely that an increase of synchronization could help to terminate seizures.

Acknowledgements

Kaspar Schindler was supported by a scholarship of the SSMBS (Schweizerische Stiftung für Medizinisch-Biologische Stipendien) donated by Roche. Christian E. Elger and Klaus Lehnertz acknowledge support from the Deutsche Forschungsgemeinschaft (SFB TR3).

References

- Bernard C. Dogma and dreams: experimental lessons for epilepsy mechanism chasers. *Cell Mol Life Sci* 2005;62:1177–81.
- Caspers H, Speckmann EJ. Cerebral pO₂, pCO₂, and pH: changes during convulsive activity and their significance for spontaneous arrest of seizures. *Epilepsia* 1972;13:699–725.
- Chen WY, Wasterlain CG. Status epilepticus: pathophysiology and management in adults. *Lancet Neurol* 2006;5:246–56.
- Cobb SR, Buhl EH, Halasy K, Paulsen O, Somogyi P. Synchronization of neuronal activity in hippocampus by individual GABAergic interneurons. *Nature* 1995;378:75–8.
- Engel JJ, Van Ness P, Rasmussen T. Outcome with respect to epileptic seizures. In: Engel JJ, editor. *Surgical treatment of the epilepsies*. New York, NY: Raven Press; 1993. p. 609–21.
- Galderisi S, Sannita WG. Pharmaco-EEG: a history of progress and a missed opportunity. *Clin EEG Neurosci* 2006;37:61–5.
- Glass L, Josephson ME. Resetting and annihilation of reentrant abnormally rapid heartbeat. *Phys Rev Lett* 1995;75:2059–62.
- Hvidberg EF, Dam M. Clinical pharmacokinetics of anticonvulsants. *Clin Pharmacokinet* 1976;1:161–88.
- Jedlicka P, Backus KH. Inhibitory transmission, activity-dependent ionic changes and neuronal network oscillations. *Physiol Res* 2006;55: 139–49.
- Jolliffe IT. *Principal component analysis*. 2nd ed. New York: Wiley; 2002.
- Logroscino G, Hesdorffer DC, Cascino G, Hauser A, Coeytaux A, Galobardes B, et al. Mortality after a first episode of status epilepticus in the United States and Europe. *Epilepsia* 2005;46(Suppl.11):46–8.
- Milton J, Jung P. Brain defibrillators: synopsis, problems and future directions. In: Milton J, Jung P, editors. *Epilepsy as a dynamic disease*. Berlin: Heidelberg: Springer-Verlag; 2003. p. 341–52.
- Morrell M. Brain stimulation for epilepsy: can scheduled or responsive neurostimulation stop seizures? *Curr Opin Neurol* 2006;19:164–8.
- Müller M, Baier G, Galka A, Stephani U, Muhle H. Detection and characterization of changes of the correlation structure in multivar-

- iate time series. *Phys Rev E Stat Nonlin Soft Matter Phys* 2005;71:046116.
- Osorio I, Frei MG, Sunderam S, Giftakis J, Bhavaraju NC, Schaffner SF, et al. Automated seizure abatement in humans using electrical stimulation. *Ann Neurol* 2005;57:258–68.
- Schindler K, Leung H, Elger CE, Lehnertz K. Assessing seizure dynamics by analysing the correlation structure of multi-channel intracranial EEG. *Brain* 2007;130:65–77.
- Timofeev I, Steriade M. Neocortical seizures: initiation, development and cessation. *Neuroscience* 2004;123:299–336.
- Topolnik L, Steriade M, Timofeev I. Partial cortical deafferentation promotes development of paroxysmal activity. *Cereb Cortex* 2003;13:883–93.
- Van Paesschen W, Dupont P, Sunaert S, Goffin K, Van Laere K. The use of SPECT and PET in routine clinical practice in epilepsy. *Curr Opin Neurol* 2007;20:194–202.
- Young D, Dragunow M. The role of adenosine in status epilepticus. In: Wasterlain CG, Treimann DM, editors. *Status epilepticus. Mechanisms and management*. Cambridge, MA: MIT Press; 2006. p. 315–24.